

UNCLASSIFIED

Defense Technical Information Center  
Compilation Part Notice

ADP023825

TITLE: Large-Scale Quantum-Mechanical Simulations of Nanoscale Devices and New Materials

DISTRIBUTION: Approved for public release, distribution unlimited

This paper is part of the following report:

TITLE: Proceedings of the HPCMP Users Group Conference 2004. DoD High Performance Computing Modernization Program [HPCMP] held in Williamsburg, Virginia on 7-11 June 2004

To order the complete compilation report, use: ADA492363

The component part is provided here to allow users access to individually authored sections of proceedings, annals, symposia, etc. However, the component should be considered within the context of the overall compilation report and not as a stand-alone technical report.

The following component part numbers comprise the compilation report:  
ADP023820 thru ADP023869

UNCLASSIFIED

# Large-Scale Quantum-Mechanical Simulations of Nanoscale Devices and New Materials

J. Bernholc, M. Buongiorno Nardelli, W. Lu, and  
S. Nakhmanson  
Department of Physics, North Carolina State  
University, Raleigh, NC  
bernholc@ncsu.edu and {nardelli, wlu,  
nakhmans}@nemo.physics.ncsu.edu

V. Meunier  
Center for Computational Sciences (CCS) and  
Computer Science and Mathematics Division,  
Oak Ridge National Laboratory, Oak Ridge, TN  
meunierv@ornl.gov

## Abstract

*Recent advances in theoretical methods and high performance computing allow for reliable first-principles investigations of nanoscale devices and complex materials. Using large scale  $O(N)$  real-space-based ab initio calculations, we carried out a theoretical study of carbon nanotube-cluster composites as prototype systems for molecular sensing at the nanoscale. Dramatic changes in the electrical conductance of the composite are predicted when gas molecules are adsorbed onto the metal clusters. The observed sensitivity and selectivity might suggest new avenues for the design and production of nanotube-based molecular sensors. The second part of this article focuses on calculating and predicting the properties of piezoelectrics, and on “designing” new materials with enhanced piezoelectric response. We consider polymers in the polyvinylidene fluoride (PVDF) family and show that our calculations not only reproduce well the existing experimental data, but also provide a much improved understanding of their polar properties, which leads to a “design” of novel polymers with a BN backbone. The new polymers are predicted to have up to 100% better piezoelectric response and an enhanced thermal stability with respect to their PVDF analogs. Since methods for their synthesis are readily available, they offer a promising avenue for improving ferro and piezoelectric devices.*

## 1. Nanotube/Cluster Molecular Sensors

Nanotubes exhibit remarkable structural and electronic properties that are very attractive for future nanoelectronic devices. We have recently reviewed the electrical properties of nanotubes, which is a very active

field at present.<sup>[1]</sup> In our current research, we aim to identify the critical elements of nanotube-based sensors that would be ultra-fast and ultra-sensitive, ideally enabling close to single-molecule detection with high specificity. The pioneering work of Dai and co-workers<sup>[2]</sup> has already shown that the nanotube conductance is sensitive to absorbed gases: adsorbed nitrogen dioxide changes a semiconducting nanotube to a metallic one, while adsorbed ammonia opens an electronic gap in an originally metallic nanotube. A number of potential nanotube-based sensor structures have been investigated since then, including hydrogen sensors<sup>[3]</sup>, polymer-coated nanotubes<sup>[4]</sup>, FET structures for alcohol detection<sup>[5]</sup>, and organic vapor detectors.<sup>[6]</sup>

The current sensors are already very sensitive, due to their nanoscale dimensions, but do not display much specificity. Their operation is believed to rely on charge transfer between the adsorbed species and the nanotube. The electron or hole donation is detected electrically, and a small diameter of the nanotube ensures a significant response to even small perturbations. While non-specific gas sensors might still be very useful in acting as a “canary in a mineshaft,” detecting the presence of gas species in a restricted environment using more selective sensors would be far more useful. We are exploring the possibility of developing species-specific sensors by combining nanotubes with metal clusters. The idea here is to utilize well-known cluster chemistry to equip clusters with specific receptors, so that only well-defined gases or molecules would adsorb. Methods for creating and dispersing small metal clusters are also well known, and the coating of nanotubes with clusters has already been achieved by electron beam evaporation, by chemical attachment of preformed clusters, and by precipitation from metal salt solutions.

We have investigated semiconducting single-wall nanotubes in combination with  $Al_{13}$  clusters.  $Al_{13}$

assumes an icosahedral structure that needs only one electron to close its electron shell with 40 electrons. Experimentally,  $\text{Al}_{13}$  with 40 valence electrons exhibits the strongest shell closing effect and is so stable that it does not react with oxygen. Moreover, its derived binary clusters  $\text{Al}_{13}\text{X}$  or  $\text{Al}_{12}\text{X}$  ( $\text{X}=\text{Cu}, \text{Ag}, \text{Au}, \text{C}, \text{et al.}$ ) also show enhanced stability and are considered as the possible building blocks for future metal cluster crystals.<sup>[7]</sup>

Our calculations used the real-space multigrid method<sup>[8]</sup> and optimized localized orbitals<sup>[9]</sup> to evaluate the electronic transport.<sup>[10]</sup> The calculations clearly show that the effect of cluster and especially molecular adsorption on resistance is significant, see Figure 1. In particular, a semiconducting nanotube remains semiconducting after cluster deposition, even when the cluster/nanotube ratio is about 10%. However, an addition of a single ammonia molecule per Al cluster leads to substantial changes in the I/V characteristics. The nanotube becomes metallic for positive biases and ammonia adsorption can thus be easily detected electrically. This nanotube-cluster assembly displays some specificity even if no receptors are used. For example, we find that the addition of diborane onto the cluster has no substantial effect on conductance. Although it reacts strongly with the cluster, dissociating into two  $\text{BH}_3$  units and significantly distorting the structure of the cluster, it introduces only localized states in the band gap region, which do not allow for electron transmission.

Turning to metallic nanotubes, our calculations for (5,5) nanotubes demonstrate a corresponding effect, namely that the adsorption of metal clusters decreases the conductance and that the adsorption of ammonia onto the clusters results in a semiconducting nanotube-cluster assembly.

Although these calculations provide a proof of principle, additional and more detailed simulations are needed in order to assess the viability of this approach. For instance, it is much easier to fabricate stable noble-metal nanoclusters in the laboratory and their receptor chemistry is much better understood. However, we still need to test whether sufficient charge transfer occurs in these systems to provide an electrical "signature" of the adsorbed molecules. In addition, we plan to investigate the various ways in which a metal cluster can strongly attach to a nanotube and form some partially-covalent bonds. This would increase the nanotube-cluster interactions and thus the strength of the signal.

## 2. New Piezo and Ferroelectric Materials

Ferro and piezoelectric materials are an increasingly important class of solids with many potential applications.

In ferroelectric materials, the positive and negative charges are displaced with respect to each other in such a way that the electric fields due to these charges produce a net electric field inside the material. In piezoelectrics, applied stress results in a net electric field, again due to displacement of the charges. The net electric field in ferroelectric materials also changes under stress, and ferroelectrics often have large piezoelectric coefficients. Conversely, applying an electric field to a piezoelectric will result in a mechanical force and either elongation or contraction of the material in the direction of the field. Thus, piezoelectric actuators are often used when precise control over motion is necessary, e.g., in various kinds of atomic resolution microscopy, where an almost atomically sharp tip is moved over a sample, in sonar equipment, or in high fidelity speakers. Since precise control and switching is the hallmark of advanced engineering, the uses of piezoelectrics continue to expand and various advanced applications to flight control systems have also been proposed. Almost as importantly, piezoelectrics can serve as embedded strain sensors, providing crucial information about stresses in various parts of engineered structures through simple voltage readouts.

The majority of existing piezoelectrics belong to two main families: those based on tri-metal oxides containing lead, zirconium and titanium (the so-called PZT systems), and fluorine-based polymers, such as polyvinylidene fluoride (PVDF). The PZT ceramics are very strong piezo- and pyroelectrics<sup>[11]</sup> but, unfortunately, are also brittle and quite heavy. Furthermore, their lead content poses environmental problems. On the other hand, the piezoelectric polymers are lightweight, flexible and virtually inert, but their polar properties are an order of magnitude weaker than those of PZT.<sup>[12]</sup> It would of course be very desirable to identify new materials that would combine the attractive properties of PZT ceramics and the polymers. Since the DTF-based methods for investigating materials and their properties have become very reliable, we embarked on the study of new materials and structures that could potentially lead to much improved piezoelectric properties. In the previous year, we investigated boron nitride nanotubes (BNNTs). Because the bond between the boron and nitrogen atoms is polar, there should be a potential for a sizable polar field along the tube axis. In particular, model calculations using simplified quantum mechanical methods<sup>[13]</sup> predicted strong piezo- and pyroelectric effects, with the direction of the spontaneous electric field that alternates in sign as the diameter of the tubes is increased. However, our calculations show that when ionic and electronic contributions to polarization are calculated accurately, they cancel, due to the chiral symmetry of an isolated nanotube. In nanotube bundles the exact symmetry is broken, leading to weak pyroelectricity. For

example, in (7,0) bundles at equilibrium distance of 3.2 Å, polarization increases to 0.01 C/m<sup>2</sup>.

The piezoelectric properties of BNNTs are more promising. Our calculated piezoelectric constants for various bundles comprised of zigzag BNNTs range from 0.39 C/m<sup>2</sup> for (5,0) tubes with 3.9 Å diameter to 0.19 C/m<sup>2</sup> for 10.2 Å wide tubes. While these are modest when compared with the PZT-based materials, they are comparable to those of piezoelectric polymers in current use. (See also the next section.) Since BN nanotubes are extremely strong and resilient, they could be used whenever a combination of high mechanical strength and a substantial piezoelectric response is required.

### 3. Quantum Mechanical Computations of Polarization in Materials

In the modern theory of polarization, the polarization-related properties of materials can be computed with two complementing approaches: the “Berry phase” method or the localized Wannier function technique.<sup>14,15]</sup> In both cases a polarization difference  $\Delta\mathbf{P} = \mathbf{P}^{(\lambda)} - \mathbf{P}^{(\lambda_0)}$  between the two states of material is computed, with  $\lambda$  being an adiabatic transformation bringing one state to the other while leaving the system insulating.

In the Berry-phase method, the expression for the total polarization of the system, split for convenience into the ionic and electronic parts  $\mathbf{P}_{ion}^{(\lambda)}$  and  $\mathbf{P}_{el}^{(\lambda)}$ , can then be written as follows (for the paired electron spins):

$$\mathbf{P}^{(\lambda)} = \mathbf{P}_{ion}^{(\lambda)} + \mathbf{P}_{el}^{(\lambda)} = \frac{e}{V} \sum_{\tau} Z_{\tau}^{(\lambda)} \mathbf{r}_{\tau}^{(\lambda)} - \frac{2ie}{8\pi^3} \sum_{occ} \int_{BZ} d\mathbf{k} \left\langle u_{ik}^{(\lambda)} \left| \nabla_{\mathbf{k}} \right| u_{ik}^{(\lambda)} \right\rangle,$$

where  $V$  is the volume of the unit cell,  $Z_{\tau}$  and  $\mathbf{r}_{\tau}$  are the charge and position of the  $\tau$ -th atom in the cell, and  $u_{ik}^{(\lambda)}$  are the occupied cell-periodic Bloch states of the system. For the electronic part, an electronic phase  $\varphi_{\alpha}^{(\lambda)}$  (Berry phase) defined modulo  $2\pi$  can be introduced as  $\varphi_{\alpha}^{(\lambda)} = V \mathbf{G}_{\alpha} \cdot \mathbf{P}_{el}^{(\lambda)} / e$ , where  $\mathbf{G}_{\alpha}$  is the reciprocal lattice vector in the direction  $\alpha$  along which we would like to compute polarization. In a similar fashion, one can construct an angular variable for the ionic part (the “ionic” phase), so that the total geometrical phase is

$$\Phi_{\alpha}^{(\lambda)} = \sum_{\tau} Z_{\tau}^{(\lambda)} \mathbf{G}_{\alpha} \cdot \mathbf{r}_{\tau}^{(\lambda)} + \varphi_{\alpha}^{(\lambda)}.$$

The total polarization in the direction  $\alpha$  is then derived from  $\Phi_{\alpha}^{(\lambda)}$  as  $\mathbf{P}_{\alpha}^{(\lambda)} = e\Phi_{\alpha}^{(\lambda)} \mathbf{R}_{\alpha} / V$ , where  $\mathbf{R}_{\alpha}$  is the real-space lattice vector corresponding  $\mathbf{G}_{\alpha}$  to, i.e.,  $\mathbf{R}_{\alpha} \cdot \mathbf{G}_{\alpha} = 1$ . Alternatively, the electronic polarization of the system can be expressed in terms of centers of charge of Wannier

functions (WFs) of its occupied bands.<sup>[14,15]</sup>

$$\mathbf{P}_{el}^{(\lambda)} = -\frac{2e}{V} \sum_i \left\langle W_{iR}^{(\lambda)} \left| \mathbf{r} \right| W_{iR}^{(\lambda)} \right\rangle d\mathbf{r} = -\frac{2e}{V} \sum_i \left\langle \mathbf{r}_i^{(\lambda)} \right\rangle.$$

Here the WF  $W_{iR}^{(\lambda)}(\mathbf{r})$  is constructed from the Bloch states  $u_{ik}^{(\lambda)}$  of band  $i$  with the unitary transformation

$$W_{iR}(\mathbf{r}) = \frac{V}{(2\pi)^3} \int_{BZ} u_{ik}(r) e^{i\mathbf{k} \cdot \mathbf{R}} d\mathbf{k},$$

and  $\left\langle \mathbf{r}_i^{(\lambda)} \right\rangle$  is the center of charge for the WF  $W_{iR}^{(\lambda)}$ . The localized WFs can be computed by a number of different techniques, for example, by minimizing the sum of the quadratic spreads of the Wannier probability distributions<sup>[16,17]</sup>

$$\Omega = \sum_j \left( \left\langle W_{i0} \left| r^2 \right| W_{i0} \right\rangle_j - \left\langle W_{i0} \left| \mathbf{r} \right| W_{i0} \right\rangle_j^2 \right).$$

In either approach (Berry phases or localized WFs), due to the arbitrariness in the choice of the phases of the Bloch functions,  $\mathbf{P}_{el}^{(\lambda)}$  can be obtained only modulo  $2e\mathbf{R}/V$ . However, the difference in polarization  $\Delta\mathbf{P}$  remains well defined provided that  $|\Delta\mathbf{P}_{el}| \ll |2e\mathbf{R}/V|$ .

### 4. Superpolar Polymers by Design

Polymers based on polyvinylidene fluoride (PVDF),  $[-\text{CH}_2-\text{CF}_2-]_n$ , are the most well known and widely used family of polymer ferroelectrics. PVDF can be grown in a variety of phases that usually are only partially crystalline. The structure of the most polar  $\beta$  phase of PVDF is shown in Figure 2(a). The maximum value of polarization in this phase is obtained due to a highly ordered arrangement of intrinsically polar  $[-\text{CH}_2-\text{CF}_2-]$  monomers. Each VDF monomer has a non-zero dipole moment, directed perpendicular to the carbon backbone, which is the sum of the dipole moments of the F-C and C-H bonds. Our calculated values of the polarization dipoles are shown in Figure 2 and also given in Table 1.

Unfortunately,  $\beta$ -PVDF can currently be grown only ~50% crystalline, which dilutes its polar properties. However, PVDF copolymers with tri-fluoroethylene (TrFE),  $[-\text{CHF}-\text{CF}_2-]$ , and tetra-fluoroethylene (TeFE),  $[-\text{CF}_2-\text{CF}_2-]$ , shown in Figure 2b, can be grown up to 90% crystalline. Because of their high crystallinity, they often exhibit better properties than “pure”  $\beta$ -PVDF, even though individual TrFE and TeFE monomers are less polar than VDF. Still, spontaneous polarization and piezoelectric response in all these materials are much weaker than in perovskite ferroelectrics. It would of course be highly beneficial to find a way to improve the polar properties of these polymers, while retaining their

superb mechanical properties and low environmental impact.

However, although the above “bond-dipole” argument provides a potentially important suggestion for improving the properties of PVDF-like materials, it can neither reliably assess the *magnitude* of such improvements nor evaluate whether the improved material would be stable. The DFT-based methods for computing structural and polar properties, however, allow us to do just that: make accurate *quantitative* predictions about the stability of the proposed material as well as the polarization and piezoelectricity improvement in our “structure by design.”

**Table 1. Polar properties of the PVDF polymer family and the BN-based “structures by design”. All polymer models are 100% crystalline. Spontaneous polarization  $P_3^{sp}$  and piezoelectric stress constants  $e_{3i}$  are given in the units of C/m<sup>2</sup>. Experimental results, shown for comparison, are extrapolated to 100% crystallinity and rescaled for the 75/25 mol% content where indicated.**

	$P_3^{sp}$	$e_{31}$	$e_{32}$	$e_{33}$	Comment
$\beta$ -PVDF	0.178 (0.131)	-	-	-	calculation with noninteracting dipoles
P(VDF/TrFE) (75/25)	0.128 (0.123)	-	-	-	experiment
P(VDF/TeFE) (75/25)	0.104 (0.118)	-	-	-	experiment
PADFB	0.362	-	-	-	
		0.493	0.580	0.555	
PAB	0.300	-	-	-	
		0.348	0.398	0.431	
PbTiO <sub>3</sub> crystal	0.88	-0.93		3.23	calculation with DFT and Berry phases

In fact, due to its simple structure,  $\beta$ -PVDF can serve as a “template” for the design of advanced polymer materials. We can use a simple “bond-dipole” picture of polarization of Figure 2 to obtain clues about possible PVDF-like structures that could have improved polarization. For example, we can make the fluorine end of the VDF monomer more negative if the carbon in the F-C bonds is replaced by a less electronegative atom. In the same fashion, the hydrogen end of the monomer will become more positive if a more electronegative atom than carbon participates in the hydrogen bonds. Taking a hint from the close analogy between the carbon and BN nanotube structures, let us consider the replacement of the carbon backbone with that of boron nitride. If the C atom at the bottom of the monomer is replaced with B and the one on the top with N, the polarity of both F-B and N-H bonds should be magnified, thereby enhancing the dipole

moment per monomer. The resulting  $[-BF_2-NH_2-]_n$  polymer is called polyaminodifluoroborane (PADFB), but an even simpler structure,  $[-BH_2-NH_2-]_n$  polyaminoborane (PAB), the BN analogue of polyethylene, should become piezoelectric and pyroelectric. The monomers of both of these structures are shown in Figure 2c.

The results of our calculations<sup>[18]</sup> of spontaneous polarization and piezoelectricity for the PVDF polymer family and its BN-based analogs are presented in Table 1, together with comparisons to experimental data, where available. Unfortunately, for pure  $\beta$ -PVDF, its low crystallinity in currently available samples prevents a meaningful comparison with the data. In particular, we find a significant polarizing effect due to interaction between polymer chains. For isolated, individual PVDF chains the dipole moment per monomer is 2 Debye, but it increases to 3 Debye when fully aligned chains are assembled into a  $\beta$ -PVDF crystal. The major part of this improvement comes from redistribution of the electron charge as the chains are brought closer together and only a minor part is due to ionic movement. However, for highly crystalline PVDF copolymers a comparison with experimental data can be made, and it shows an excellent agreement with our calculations for both TrFE and TeFE structures. This effectively validates our approach of computing polarization in polymeric materials and provides credibility for the predictions regarding the “designed” BN-based polymers, where no experimental data is available. As we expected, the BN backbone leads to a substantial increase in polarization. For PADFB, the polarization is raised by 100%, compared to  $\beta$ -PVDF, which also results in a nearly twofold enhancement in the piezoelectric properties. For PAB, we obtain a more modest increase in spontaneous polarization, accompanied by an appropriate improvement in piezoelectricity.

An additional consideration in the design of polymers is the stability of their ordered polar phases. We therefore computed the chain-rotation barriers for all of the polymers discussed above, since the ordered phase is usually destroyed via random, thermally-induced chain rotations. PAB, which does not contain fluorines, is significantly less stable than  $\beta$ -PVDF, with a low chain-rotation barrier of 0.28 eV per monomer. However, the height of the barrier in PADFB is about 2.4 eV per monomer, more than three times larger than in  $\beta$ -PVDF (0.72 eV), indicating that the polar phase in PADFB should be much more stable than in  $\beta$ -PVDF. The last result is consistent with the experimental evidence of increased thermal stability of PADFB.

It is both surprising and very encouraging that both of the BN-based polymers are already well-known, although to the best of our knowledge their polar properties have not been investigated. PAB, for example, is routinely

employed as a precursor for preparing hexagonal boron nitride. PADFB has also been synthesized, although not in large quantities, but there are indications in the literature that developing such a process would be relatively straightforward<sup>[19]</sup>. However, as grown, these polymers are unlikely to be ordered and thus highly ferro and piezoelectric. In fact, the well-known PVDF-based polymers must be stretched and poled after growth to form ordered structures with non-zero macroscopic polarization. The increased chain-rotation barriers of BN-based polymers will make both the ordering and disordering transformations more difficult, and advanced growth and processing methods may be needed before highly polar samples are produced. However, the large improvement in the ferro and piezoelectric constants, combined with the excellent mechanical and environmental properties inherited from PVDF, makes these polymers highly attractive targets for future experimental studies and potential high value applications.

## References

- Bernholc, J., D. Brenner, M. Buongiorno Nardelli, V. Meunier, and C. Roland, *Annual Rev. Mat. Sci.*, 32, 2002, pp. 347–75.
- Kong, J., N.R. Franklin, C.W. Zhou, M.G. Chapline, S. Peng, K.J. Cho, and H.J. Dai, *Science*, 287, 2000, p. 622.
- Kong, J., M.G. Chapline, and H. Dai, *Adv. Mater.*, 13, 2001, p. 1384.
- Qi, P., O. Vermesh, M. Grecu, A. Javey, Q. Wang, and H. Dai, *Nano Lett.*, 3, 2003, p. 347.
- Someya, T., J. Small, P. Kim, C. Nuckolls, and J.T. Yardley, *Nano Lett.*, 3, 2003, p. 877.
- Li, J., Y. Lu, M. Cinke, J. Han, and M. Meyyappan, *Nano Lett.*, 3, 2003, p. 929.
- Gong, X.G. and V. Kumar, *Phys. Rev. Lett.*, 70, 1993, 14.
- Briggs, E.L., D.J. Sullivan, and J. Bernholc, *Phys. Rev. B*, 54, 1996, p. 14362.
- Fattebert, J.-L. and J. Bernholc, *Phys. Rev. B*, 62, 2000, p. 1713.
- Buongiorno Nardelli, M., J.-L. Fattebert, and J. Bernholc, *Phys. Rev. B*, 64, 2001, p. 245423.
- See, for example, G. Sághi-Szabó, R.E. Cohen, and H. Krakauer, *Phys. Rev. B*, 59, 1999, p. 12771.
- See, for example, *Ferroelectric polymers: chemistry, physics and applications*, edited by H.S. Nalwa Marcell Dekker, New York, 1995.
- Mele, E.J. and P. Král, *Phys. Rev. Lett.*, 88, 2002, p. 056803.
- King-Smith, R.D. and D. Vanderbilt, *Phys. Rev. B*, 47, 1993, p. 1651.
- Resta, R., *Rev. Mod. Phys.*, 66, 1994, p. 899.
- Marzari, N. and D. Vanderbilt, *Phys. Rev. B*, 56, 1997, p. 12847.
- Gygi, F., J.-L. Fattebert, and E. Schwegler, *Comp. Phys. Commun.*, 155, 2003, p. 1.
- Nakhmanson, S.M., M. Buongiorno Nardelli, and J. Bernholc, *Phys. Rev. Lett.*, 92, 2004, p. 115504.
- Pusatcioglu, S.Y., H.A. McGee, Jr., A.L. Friske, and J.C. Hassler, *J. Appl. Polym. Sci.*, 21, 1977, p. 1561.

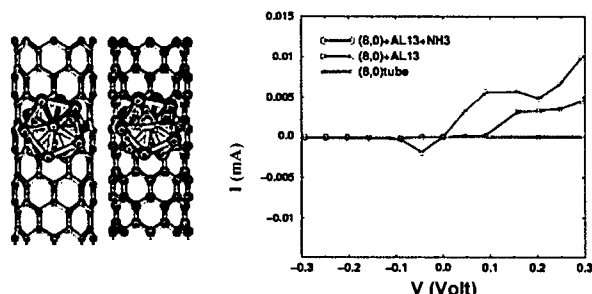


**Figure 1.** An  $\text{Al}_{13}$  cluster attached to a nanotube can serve as a chemical sensor. The left panel shows the atomic configuration before and after ammonia attachment, while the right panel displays the I/V characteristics of the nanotube-cluster-ammonia system. The ammonia attachment can be easily detected electrically. See text.

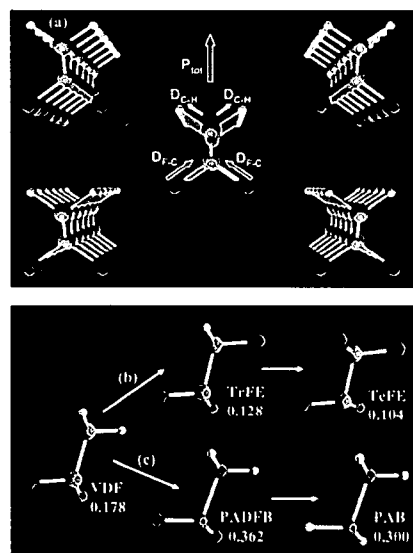


**Figure 2.** Schematic illustration of the evolution of polarization in  $\beta$ -PVDF and related polymers. (a) The structure of the crystalline  $\beta$  phase of PVDF. The F-C bond is far more ionic than the C-H bond, which leads to polarization in the VDF monomer, directed perpendicular to the carbon backbone.  $D_{F-C}$  and  $D_{C-H}$  are the bond-dipole moments. The second panel illustrates the evolution of the VDF monomer into TrFE and TeFE by substitution of the H atoms with F atoms (pathway b), and into PADFB and PAB by substitution of the carbon backbone with boron and nitrogen atoms (pathway c). The calculated spontaneous polarization for each polymer or copolymer is given in the units of  $\text{C/m}^2$ .